JOURNAL OF MATERIALS SCIENCE 29 (1994) 5014–5022

The influence of microstructure on the thermal conductivity of aluminium nitride

A. BELLOSI, L. ESPOSITO
CNR-IRTEC, Research Institute for Ceramics Technology, Faenza, Italy
E. SCAFÈ, L. FABBRI*
ENIRICERCHE, Monterotondo, Roma, Italy

Starting from three different commercial powders, AlN materials were densified by pressureless sintering under various temperature and time values in order to investigate the influence of microstructure on thermal conductivity. The influence of the sintering aids (3 wt% Y_2O_3 and 2 wt% CaC_2) and of the forming processes (cold isostatic pressing and thermocompression of tape cast pieces) were also been evaluated. Thermal conductivity increased with the purity level of the starting powder and with an increasing the sintering temperature and soaking time. The highest thermal conductivity values (196 $W m^{-1} K^{-1}$) were obtained with the purest powder and high temperature (1800 °C) sintering over long periods (6 h). No influence on thermal conductivity was detected from the forming technique.

1. Introduction

Aluminium nitride ceramics are excellent candidates for electronic applications because of their unique combination of high thermal conductivity, reasonable dielectric properties, good thermal expansion and good flexural strength [1–4].

The estimated theoretical value of their thermal conductivity at room temperature is 320 $W m^{-1} K^{-1}$. Actually, polycrystalline, AlN-based ceramics have lower thermal conductivity (from 30 to 260 $W m^{-1} K^{-1}$) [6–14]. The primary heat transport mechanism of AlN is phonon propagation. It is expected that impurities or other lattice and microstructural defects, such as vacancies, secondary phases, grain boundaries, porosity and dislocations, can cause phonon scattering and thus lower thermal conductivity.

Densification of pure AlN during sintering is difficult because of its strong covalent bond. Dense AlN materials can be achieved by using either hot pressing [12, 13] or pressureless sintering [6–16] with sintering aids such as CaO, MgO, Y_2O_3, $CaCO_3$, CaC_2, etc. Contents of 1–5 wt % of these additives are needed for full densification. It is well known that type, amounts and distribution of secondary phases deeply affect thermal conductivity values [6–23].

This study investigated the effects of AlN powder characteristics, additives, forming techniques and sintering conditions on the microstructure and thermal conductivity of AlN ceramics. Three different commercial AlN powders using two additives (CaC_2 and Y_2O_3) were densified under different conditions so as to yield large variations in phase contents, phase compositions and thermal conductivity.

2. Experimental procedure

2.1. Processing

Three commercial AlN powders: Starck grade C, Tokuyama grade G and Atochem A4 (indicated in the following as S, T and A, respectively) were tested. Powder S was produced by direct nitridation of Al. Powders T and A were produced by carbothermal reduction of Al_2O_3. The different synthesizing processes affected grain size and shape and the type and amounts of the impurities. These powders (Table I) exhibited different particle size distributions (Fig. 1) and particle shapes (Fig. 2). In particular, powder S had the highest specific surface area, a wide particle size distribution and a high percentage of submicrometre particles together with irregular and angular particle shapes. Powders T and A had a narrow particle size distribution, spherical particles and mean grain sizes of 1.9 and 1.1 μm, respectively.

From the chemical point of view, powder S had the highest impurities content (mainly oxygen and iron due to the production process), while powder T was the purest. As sintering aid Y_2O_3 (Starck, grade C) was used in an amount of 3 wt %; CaC_2 (Riedel-de Haën, C-M-Gerät) was also added to powder S in an amount of 2 wt %.

Green bodies of AlN were prepared by using two different forming methods:

1. Cold isostatic pressing (CIP) from a blend obtained by mixing AlN powder with the sintering aid in isobuthyl alcohol containing 3 wt % of organic binder using alumina milling media. After drying, the mixed powders were die pressed in cylindrical moulds

* *Present address*: CEC-Joint Research Centre, ISPRA site, ISPRA, VA, Italy.

0022–2461

TABLE I Main characteristics of the three powders

Powder		S (STARCK C)	T (TOKUYAMA G)	A (ATOCHEM A4)
Impurities (%)[a]	O	< 2.5	0.99	1.1
	C	0.08	0.04	< 0.1
	Fe	< 0.10	0.001	< 0.005
	Ca	–	150 ppm	30 ppm
	Si	–	30 ppm	50 ppm
Other metal impurities (%)[a]		0.10	–	< 30 ppm
Specific surface area[b] ($m^2\ g^{-1}$)		4.87	2.47	2.88
Mean particle size[c] (μm)		0.85	1.90	1.10
Particles < 1 μm (wt %)		60	10	45

[a] Chemical composition measured by the producer; [b] specific surface area; BET method; [c] mean particle size; from the equivalent spherical diameter.

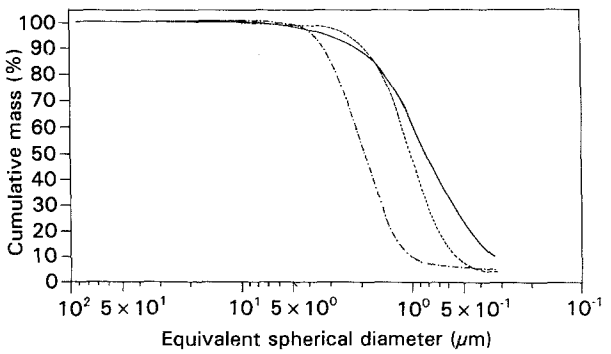

Figure 1 Grain size distribution of the three AlN tested powders. —, S; –·–, T; – – –, A.

(13 mm in diameter and 18 mm in height) under a pressure of 1000 kg cm^{-2} and subsequently cold isostatically pressed under the same pressure. The green relative densities, reported in Table II, ranged from 55 to 61% of the theoretical ones.

2. Thermocompression of tape cast (TC) specimens. The preparation of the tape casting slurry was performed by fast mixing the powders in a plastic jar with alumina balls, following these steps:

(a) addition of 80 wt % dispersant with deflocculant and Y_2O_3 powder, mixing for 2 min;

(b) addition of AlN powder in three subsequent steps, mixing for 5 min each;

(c) addition of the binder previously dispersed in the remaining 20 wt % dispersant, mixing for 10 min;

(d) addition of the plasticizer and mixing for 15 min.

The slurry was then degassed to eliminate air bubbles and then tape cast. Cylindrical samples of 13 mm diameter and 15 mm height, were realized with discs stamped from the tape and thermocompressed at 120 °C under a pressure of 500 kg cm^{-2}.

Burn-out cycles for all the three tape cast materials were performed in air up to 600 °C. Weight losses of 13 wt % were found, corresponding to all of the organic phases and traces of carbon present as powder impurities. The green relative densities reported in Table II varied from 55 to 60% of theoretical ones.

For densification, the AlN green bodies were placed in a BN lined graphite crucible and embedded in a protective packing powder (80 wt % BN, 20 wt % AlN). A sintering temperature ranging from 1700 to 1900 °C was chosen with various soaking times (1–6 h) and under a flowing nitrogen atmosphere.

2.2. Microstructure characterization

The AlN microstructure was characterized using scanning electron microscopy (SEM) to evaluate grain size and shape, grain boundaries and porosity on polished and fractured surfaces. An energy-dispersive X-ray spectrometer (EDS) attached to an SEM was used in order to characterize the chemical composition of the grain boundaries.

2.3. Evaluation of thermal conductivity

The thermal conductivity (κ) was calculated from $\kappa = \rho\alpha c_p$, where ρ is density measured using the water immersion method, c_p is heat capacity (data from the literature) and α is thermal diffusivity measured by using the laser flash method. The following experimental set-up was used. A 50 J Nd/glass laser (Lumonics Ltd), with a pulse width of ca. 500 μs and a wavelength of 1.06 μm, was used as the pulse source. The laser intensity was attenuated by a copper sulphate solution designed to keep the sample rear-surface temperature rise below 1 K and to avoid a temperature dependence effect [24]. The laser beam diameter was expanded to ca. 15 mm by using a suitable lens system, and a fraction of its intensity was masked off before hitting the sample. The uniformity of the beam was tested using footprint pattern paper after strong attenuation of the laser pulse to control non-uniform heating effects [25].

The average temperature rise of the sample rear-surface was measured by using an InSb infrared detector (EG&G Judson, J10D-M204-R04M 60). It had two windows of sapphire and germanium connected to its sensitive surface which were designed to cut off radiation at 8 and 2 μm. The signal was pre-amplified (EG&G Judson PA-9-44) and then transmitted to a low-noise amplifier (Stanford Res. Sys., SR 560) with variable gain and filtering. Then the signal was recorded by an accurate (12 bit) digitizing oscilloscope (Hewlett Packard, 5183 T) and fed to a personal computer via an IEEE-488 bus programmed to control the apparatus and to sample 8192 data points. The 1024-

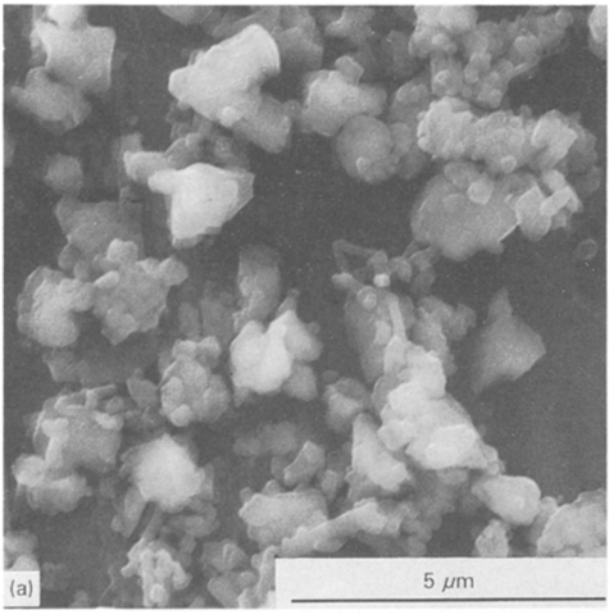

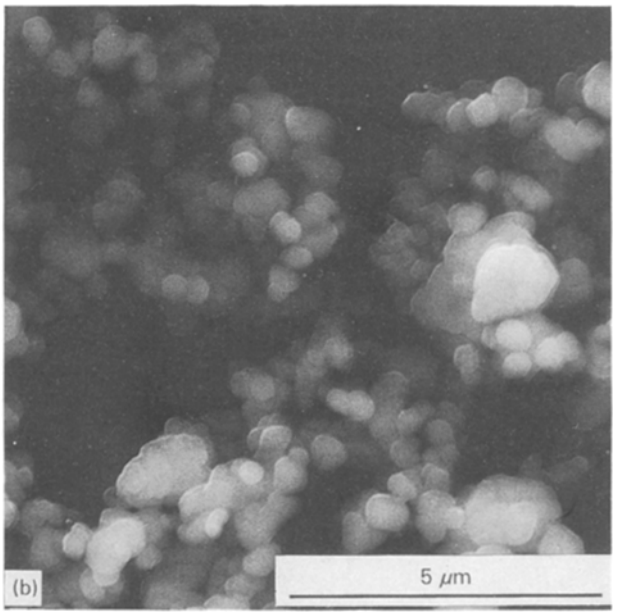

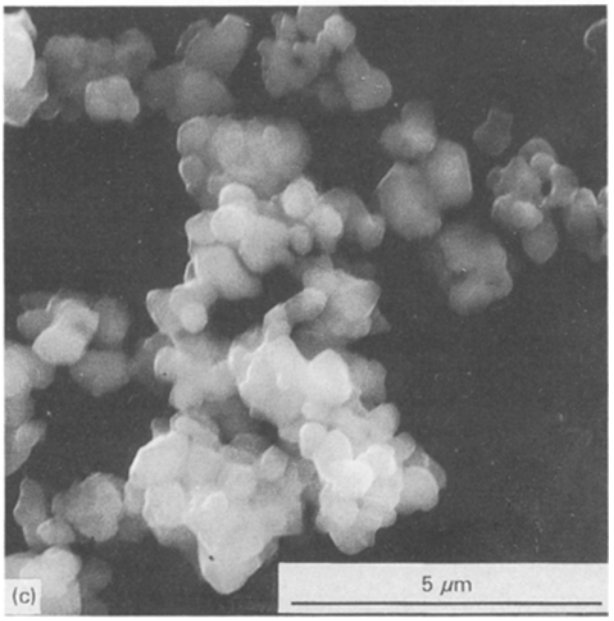

Figure 2 SEM micrographs of the three AlN tested powders (a) S; (b) T; (c) A.

TABLE II Values of green densities obtained from AlN powders with different forming techniques

Powder	Forming technique[a]	Green density ($g\ cm^{-3}$)	Green density (%)
Starck + CaC_2	CIP	1.73	54.8
Starck + Y_2O_3	CIP	1.83	55.3
Starck + Y_2O_3	TC	1.97	59.8
Atochem + Y_2O_3	CIP	1.82	55.0
Atochem + Y_2O_3	TC	1.80	54.4
Tokuyama + Y_2O_3	CIP	2.03	61.0
Tokuyama + Y_2O_3	TC	1.85	60.0

[a] CIP, isostatic pressed powder; TC, thermocompressed tape.

point experimental curve used to calculate thermal diffusivity was obtained by averaging all experimental noise to allow measurements of low temperature rises. Thermal diffusivity was then calculated both by measuring the fractional time rises (10–90%) and by using a least-square analysis; the data agreed within 1%. The samples used for the measurements were cylindrical with a diameter of 10 mm and a thickness of 4 mm. The samples were coated on both sides with a sputtered gold layer to prevent direct transmission of the laser beam. A thin coating of colloidal carbon was deposited on the top of the gold layer to enhance the adsorption of the laser beam and increase the emissivity of the monitored face.

3. Results

3.1. Densities

Sintered densities of AlN samples under different firing conditions are summarized in Tables III–V. In each case very high densities (> 97%) were obtained, but the best results were found with short sintering cycles (1–3 h at 1750–800 °C). Longer soaking times caused porous edges and scarce surface finish. As in previous studies, these problems resulted from the combination of a carbon-reducing atmosphere in the graphite die with the occurrence of some surface depletion of grain-boundary phases, in spite of the protective action of BN–AlN packing powder.

The highest densities of 99–100% were obtained at 1800 °C for 2 h with powders T and A and at 1800 °C for 1 h with powder S. The final density for all the three powders was independent of the forming process used.

3.2. Thermal conductivities

The thermal conductivity of AlN samples is summarized in Tables III–V. These values were related to four different parameters: 1. AlN powder source; 2. sintering additives; 3. forming processing; 4. firing conditions (temperatures and soaking times).

TABLE III Final characteristics of AlN based ceramics produced from Starck powder with 3 wt % Y_2O_3 or 2 wt % CaC_2

Sint. temp. (°C)	1750	1750	1750	1750	1750	1800	1800	1800	1800	1800	1800	1800	1900	1900
Sint. time (h)	4	4	4	6	6	1	1	2	2	4	4	6	6	1	1
Sint. additive	CaC_2	Y_2O_3	Y_2O_3	CaC_2	Y_2O_3	CaC_2	Y_2O_3	CaC_2	Y_2O_3	CaC_2	Y_2O_3	CaC_2	Y_2O_3	CaC_2	Y_2O_3
Forming tec.[a]	CIP	CIP	TC	CIP	CIP	CIP	CIP	CIP	CIP	CIP	CIP	CIP	TC	CIP	CIP
Density (g cm^{-3})	3.14	3.29	3.24	3.16	3.26	3.25	3.20	3.31	3.17	3.27	3.20	3.28	3.22	3.28	3.23	3.18	3.31
Density (%)	97.0	99.4	97.9	97.8	98.5	98.2	99.0	100	98.1	98.0	99.0	99.1	99.7	99.1	97.6	98.4	100
Crystalline phases	$CaAl_4O_7$	$Al_5Y_3O_{12}$	$Al_5Y_3O_{12}$	$CaAl_4O_7$ $CaAl_2O_4$	$Al_5Y_3O_{12}$	$Al_5Y_3O_{12}$	–	–	$CaAl_4O_7$	$Al_5Y_3O_{12}$	$CaAl_4O_7$	$Al_5Y_3O_{12}$	$CaAl_4O_7$	$Al_2Y_4O_9$	$Al_2Y_4O_9$		
Mean grain size (μm)	1.3	4.5	4.5	1.6	6.0	6.0	1.3	2.1	1.4	4.5	1.9	–	2.4	10.0	10.0	3.0	3.0
T. diffusivity ($cm^2 s^{-1}$)	0.34	0.32	0.329	0.34	0.33	0.35	0.22	0.28	0.33	0.35	0.37	0.36	0.38	0.39	0.61	0.27	0.26
T. conductivity ($W K^{-1}$)	84.1	84.3	85	84.1	86.1	92	52.9	68.4	82.5	91.1	92.7	94.5	94.9	103.1	158	64.7	64.2

[a] CIP, isostatic pressed powders; TP, thermocompressed tapes.

3.2.1. AlN powders

The thermal conductivity of AlN samples prepared from powder sources S, T and A were quite different, although all achieved very high densities. The plot in Fig. 3 compares the results of the samples with the same formulation (3 wt % Y_2O_3), processed and sintered under the same conditions.

Samples prepared from powder T had the highest thermal conductivity values, samples from powder S had the lowest ones. These differences were directly related to the different oxygen and metallic impurity content of the starting AlN powders. As shown in Table I, powder T was the purest powder and powder S had the highest amount of oxygen and metallic impurities.

3.2.2. Sintering aids

The influence of two different sintering aids (Y_2O_3 and CaC_2) was tested only on samples produced from powder S. Table III shows a general trend indicating that AlN with the addition of Y_2O_3 had a slightly higher thermal conductivity than samples containing CaC_2.

3.2.3. Forming technologies

In most cases the forming technology had no influence on thermal conductivity. The variations in the measured values were assumed to be associated with the general microstructural characteristics (discussed in Section 3.3).

3.2.4. Firing conditions

Fig. 3 shows that a long sintering time could yield high thermal conductivity. This effect was strongly evident only at high sintering temperatures (1800 °C): the thermal conductivity of sample T increased from 131 to 196 $W m^{-1} K^{-1}$ with an increase in sintering time from 3 to 6 h. A similar effect was observed for sample A and, to a limited degree, also for sample S.

By contrast, when sintering at 1750 °C, only a slight increase in thermal conductivity was observed with an increase in sintering time. The same effect was observed in the samples containing Y_2O_3 and CaC_2.

3.3. Microstructure

X-ray phase analyses showed in addition to AlN, some low amounts of grain boundary crystalline phases. In the samples produced from powder S containing CaC_2 as sintering aid, very small amounts of two phases ($CaAl_4O_7$ and $CaAl_2O_4$) were detected, depending on sintering temperature and time. For sintering cycles at 1750 °C for 4 h and at 1800 °C for 1 and 2 h $CaAl_4O_7$ only was found. For longer soaking times $CaAl_2O_4$ was also identified. $Al_5Y_3O_{12}$ was detected as a crystalline grain-boundary phase in samples containing Y_2O_3 as sintering aid and densified at 1750 °C for 2, 4 and 6 h, and at 1800 °C for 2 and 3 h. For longer soaking times at 1800 °C, $Al_2Y_4O_9$ was found. No differences in the crystalline grain-

TABLE IV Final characteristics of AlN-based ceramics produced by Tokuyama powder with 3 wt % Y_2O_3

Sintering temp. (°C)	1750	1750	1750	1750	1750	1750	1800	1800
Sintering time (h)	2	2	4	4	6	6	3	6
Forming technique[a]	CIP	TC	CIP	TC	CIP	TC	CIP	CIP
Density (g cm^{-3})	3.26	3.26	3.27	3.29	3.28	3.26	3.28	3.25
Density (%)	98.5	98.5	98.8	99.4	99.1	98.5	99.1	98.2
Crystalline phases	$Al_5Y_3O_{12}$	$Al_5Y_3O_{12}$	$Al_5Y_3O_{12}$	$Al_5Y_3O_{12}$	$Al_5Y_3O_{12}$	$Al_5Y_3O_{12}$	$Al_5Y_3O_{12}$	$Al_5Y_4O_9$ $Al_2Y_4O_9$
Mean grain size (μm)	3.3	3.3	3.9	3.9	5.1	5.1	4.8	6.3
T. diffusivity ($cm^2\ s^{-1}$)	0.489	0.451	0.455	0.488	0.503	0.463	0.498	0.755
T. conductivity ($W\ m^{-1}\ K^{-1}$)	128	118	123	128	132	121	131	196

[a] CIP, cold isostatic pressed powders; TP thermocompressed tapes.

TABLE V Final characteristics of AlN-based ceramics produced from Atochem powder with 3 wt % Y_2O_3

Sintering temp. (°C)	1750	1750	1750	1750	1800	1800	1800	1800	1800	1800
Sintering time (h)	2	4	6	6	2	2	3	3	6	6
Forming tech.[a]	CIP	CIP	CIP	TC	CIP	TC	CIP	TC	CIP	TC
Density (g/cm^{-3})	3.26	3.28	3.25	3.25	3.28	3.29	3.28	3.28	3.21	3.23
Density (%)	98.5	99.1	98.2	98.2	99.1	99.4	99.1	99.1	96.0	97.6
Crystalline phases	$Al_5Y_3O_{12}$	$Al_5Y_3O_{12}$	$Al_5Y_3O_{12}$	$Al_5Y_3O_{12}$	$AlYO_3$	$AlYO_3$	$Al_5Y_3O_{12}$	$Al_5Y_3O_{12}$	$Al_2Y_4O_9$	$Al_5Y_3O_{12}$ $Al_2Y_4O_9$
Mean grain size (μm)	3.8	4.5	5.4	5.4	4.5	4.5	5.1	5.1	8.5	8.5
T. diffusivity ($cm^2\ s^{-1}$)	0.436	0.402	0.408	0.406	0.417	0.434	0.489	0.453	0.686	0.654
T. conductivity ($W\ m^{-1}\ K^{-1}$)	114	106	106	106	109	114	128	119	176	169

[a] CIP, isostatic pressed powders; TP, thermocompressed tapes.

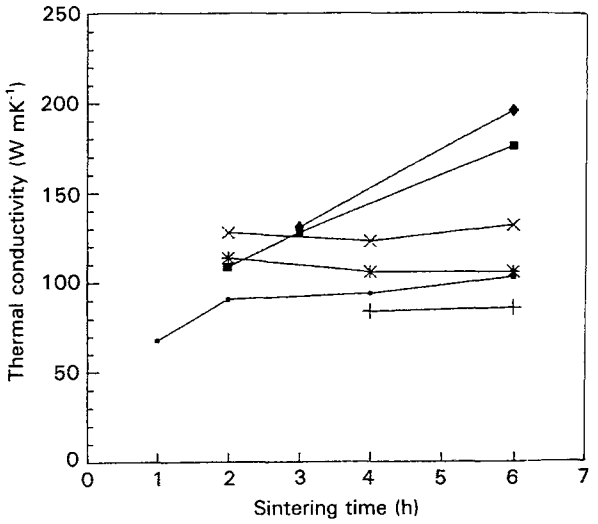

Figure 3 Plot of thermal conductivity against sintering time for different sintering temperatures of the three AlN samples. + +, 1750 °C, S; ●—●, 1800 °C, S; ✳—✳, 1750 °C, A; ×—×, 1750 °C, T; ■—■, 1800 °C, A; ◆—◆, 1800 °C, T.

boundary phases were associated with the forming process.

The above considerations must be related to the size and morphology of AlN grains and to the grain-boundary phase. Fig. 4 shows SEM microstructures of the fracture surfaces of samples S, T and A after sintering under the same firing conditions (1750 °C for 4 h). The fracture surfaces of both samples T and A revealed sharp-edged grains and small amounts of grain-boundary phases in the narrow grain boundaries and a slightly higher mean grain size for sample A. The fracture surface of sample S showed more grain-boundary phase and wider grain boundaries.

The effect of the sintering aids on the microstructure of AlN samples prepared from powder S can be observed in Fig. 5. The microstructure of AlN containing yttria was not as uniform as that containing CaC_2: sharper grain-boundary edges and clean grain boundaries indicated a much smaller amount of grain-boundary phase in AlN ceramics when CaC_2 is added. Intragranular fractures were found in the AlN sample with Y_2O_3, but no intragranular fracture was observed in the AlN sample containing CaC_2.

The effect of the sintering time on the microstructure of AlN prepared from the three powders can be observed by comparing Figs 6 and 4 (samples sintered at 1750 °C for 1 and 4 h) and Figs 7 and 8 (samples sintered at 1800 °C for 2 and 6 h). A different microstructural development was evident when comparing sample S with samples T and A. For samples produced with powder A and T the level of the grain-boundary phase was generally reduced during the

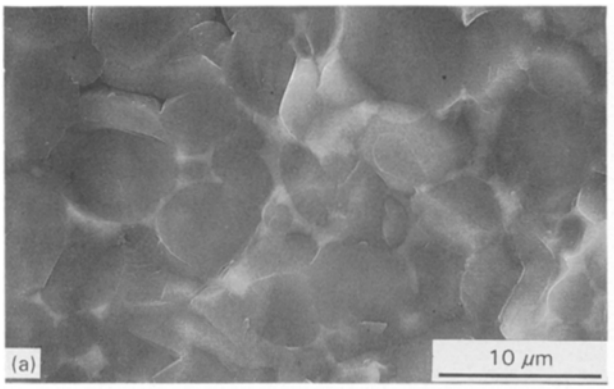

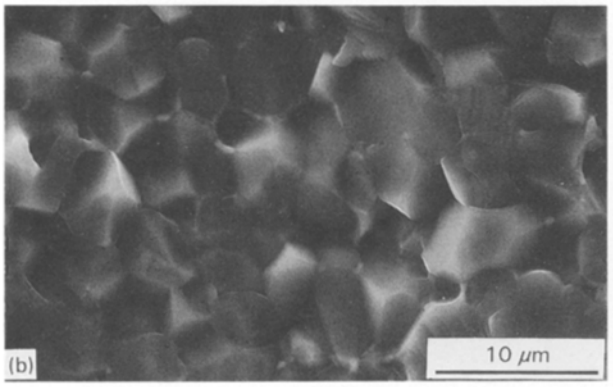

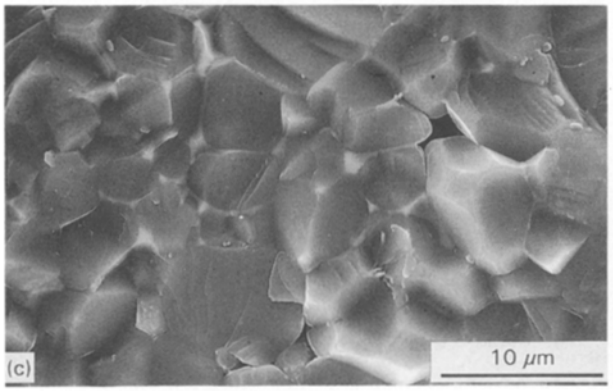

Figure 4 SEM micrographs of S (a), T (b) and A (c) samples sintered at 1750 °C for 4 h.

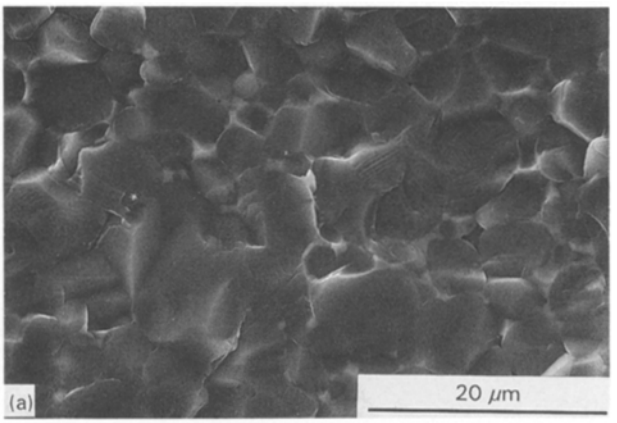

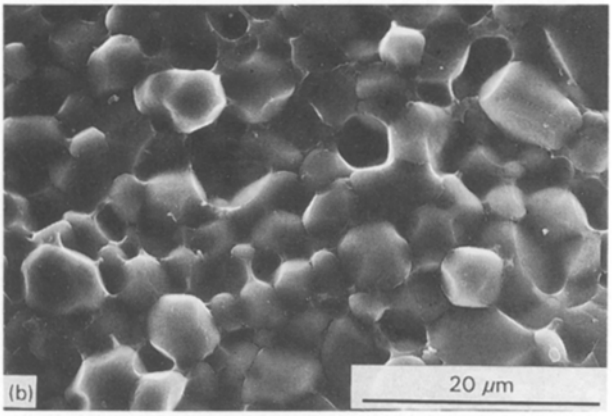

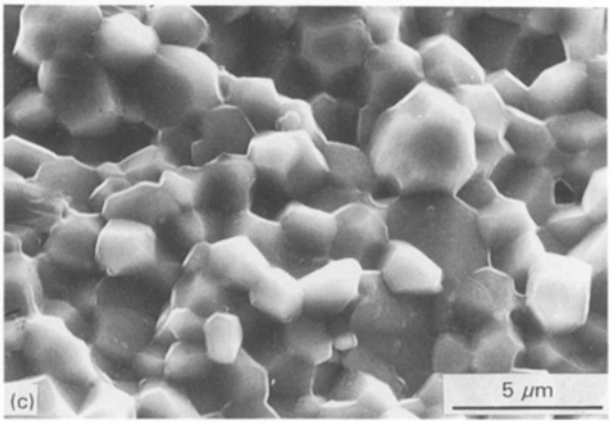

Figure 5 SEM micrographs of S (a), T (b) and A (c) samples sintered at 1750 °C for 1 h.

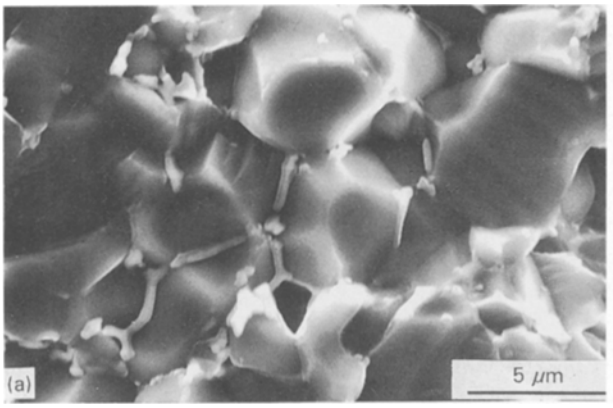

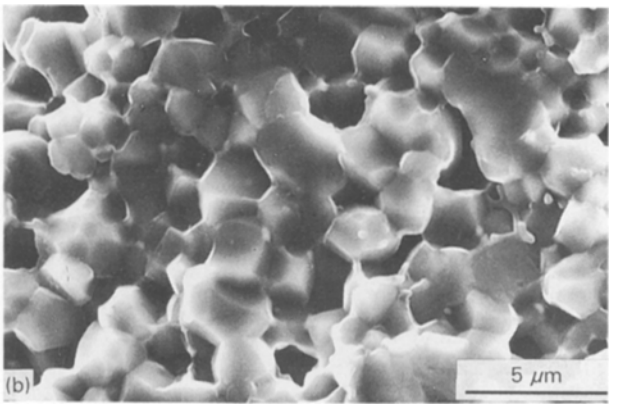

Figure 6 SEM micrographs of sample S sintered at 1800 °C for 2 h containing Y_2O_3 3 % wt (a) and CaC_2 2 % wt (b).

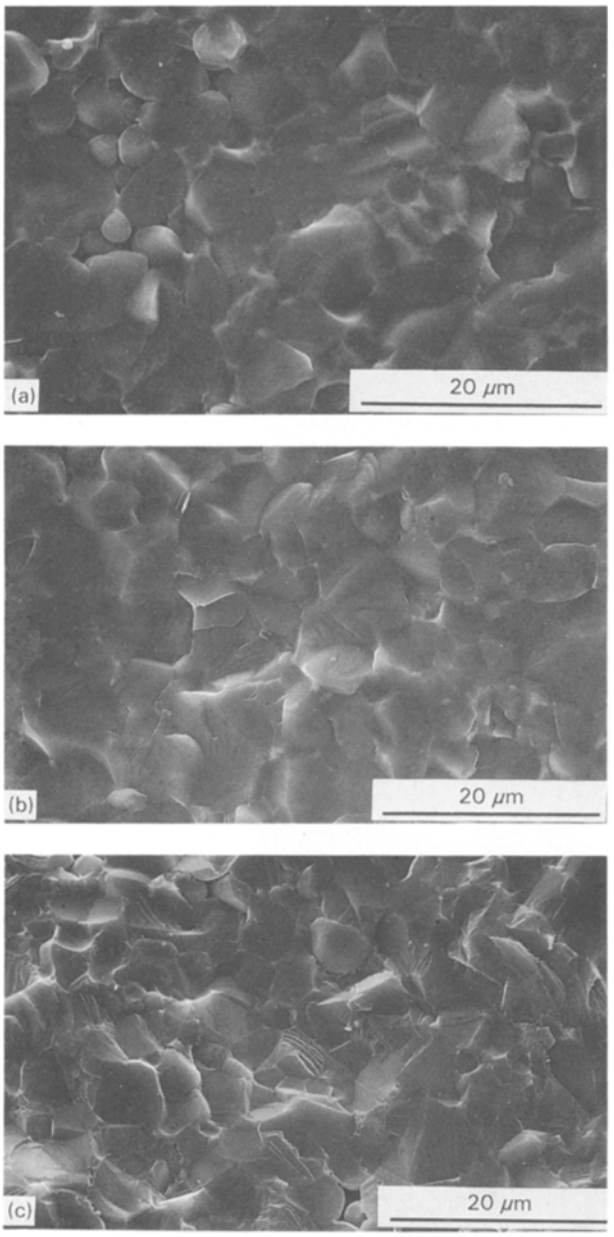

Figure 7 SEM micrographs of S (a), T (b) and A (c) samples sintered at 1800 °C for 2 h.

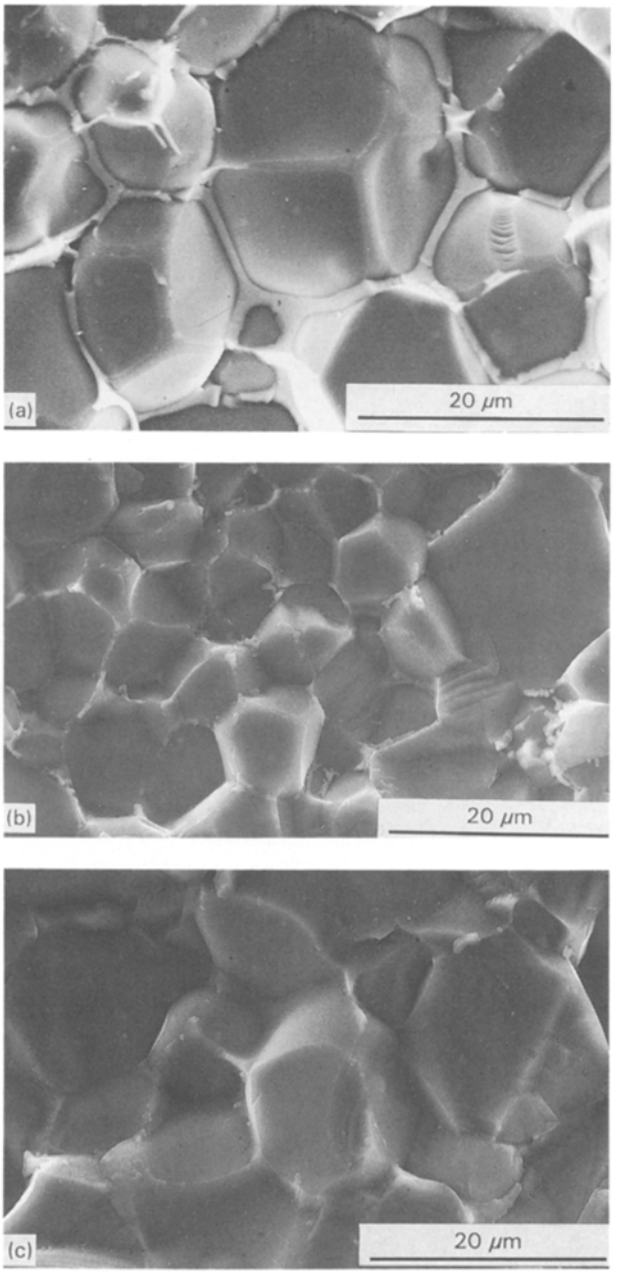

Figure 8 SEM micrographs of S (a), T (b) and A (c) samples sintered at 1800 °C for 6 h.

long holding at sintering temperature. The grain-boundary phase (yttrium aluminates) in materials produced with powder T was present as a thin layer between the AlN grains and was mainly concentrated at the corners of the polyhedra. In some cases, particularly in samples produced with powder A, AlN grains were well rounded (Fig. 8) and occasionally in close contact with one another. The yttrium aluminates generally formed grain boundary layers extending from the triple junctions. The AlN growth was very limited in the sample produced with powder T, and was more evident in samples produced with powders A and S.

In the samples produced from powder S after a long sintering cycle, there was an increased amount of the grain-boundary phase; channels which contained the oxide phases and connected the rounded corners of polyhedra were formed along the grain edges (Fig. 8). The final AlN grains were much larger than in the other cases.

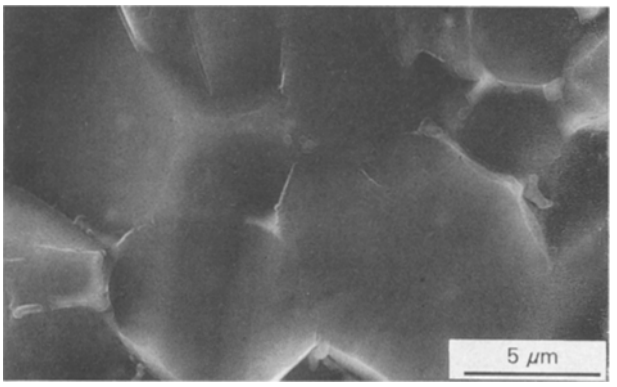

Figure 9 SEM micrograph of T sample sintered at 1800 °C for 6 h.

The sample with the highest thermal conductivity (196 $W m^{-1} K^{-1}$), prepared from powder T (Fig. 9), revealed some residual traces of grain-boundary phase and the edges of the grains were in close contact and

clean. The grain morphology was regular and relatively fine.

4. Discussion

The thermal conductivities for all materials processed were lower than the theoretical ones. However, in samples containing Y_2O_3 as a sintering aid, conductivity generally increased when the highest processing temperatures and holding times were used. As, also previously observed [6–11], thermal conductivity was related to microstructural characteristics, in particular to the volume and composition of the grain-boundary phase, to grain size and also to some lattice defects (stacking faults, dislocations and accumulations of alumina vacancy clusters). Moreover, the effect of porosity under 2 wt % could be considered irrelevant [6]. It is well known that the volume fraction of the grain-boundary phase is controlled either by the content of oxygen and impurities in the AlN starting powders which are responsible for lattice defects, such as aluminium vacancies and dislocations, or by the amount of the sintering aid.

During this study, the same amount of yttria was added as a sintering aid to all three AlN powders; therefore, the difference in the volume fraction of grain boundaries was related to the differences in oxygen and impurity content in the starting AlN powders.

The microstructures revealed a lower amount of grain-boundary phase in the samples produced by powders T and A. Moreover, it has been previously ascertained [6] that another role of oxygen and metallic impurities is to cause more lattice defects inside the grains. The difference in amount and distribution of the grain-boundary phase among these samples is related to the oxygen and impurity levels in the AlN starting powders. In powder S, the amount of impurities was relatively high and more yttrium aluminate garnet formed as part of the grain-boundary phase. Moreover, the presence of high amounts of liquid phase during sintering was the cause of the grain growth. The characteristics of the grain-boundary phases changed continuously during sintering because of an external reaction with the carbon-rich furnace atmosphere. The observed variations of crystalline grain-boundary phases from $Al_5Y_3O_{12}$ (Al_2O_3:Y_2O_3, 3:5) towards $Al_2Y_4O_9$ (Al_2O_3:Y_2O_3, 2:1) with an increase in sintering temperature and holding time, indicated a continuous depletion of oxygen and of Al_2O_3 within the grain-boundary phase owing to a carbothermal nitridation reaction of small amounts of Al_2O_3 [16]. According to the overall reaction, following the variation of the composition of the grain-boundary phases from alumina-rich to yttrium aluminate-rich ones, the purification of AlN grains took place because of the adjustment of the internal equilibrium between AlN, which contained some Al_2O_3 in solid solution, and the yttrium aluminates at the grain boundaries.

Therefore, an increase in sintering time and temperature increased thermal conductivity. As previously observed, this was strictly related to oxygen concentration in the AlN lattice [11]. Only sample S showed an apparent higher amount of grain-boundary phase after long sintering times, but its composition allowed it to obtain fairly satisfactory values of thermal conductivity (158 $W m^{-1}K^{-1}$).

Another effect, more evident at higher sintering temperatures (1900 °C) was a fast migration of the secondary phase towards the sample surface, which left some open channels and gaps among the grains.

The resultant trend towards increasing thermal conductivity with grain size may imply a grain size effect. Actually the diffusion distance from an aluminium vacancy in the AlN grain to a grain-boundary sink is shorter in smaller grains. Simultaneous long sintering times allowed more aluminium vacancies to migrate to the grain boundary. Therefore, the final phenomena was governed by the simultaneous actions of various competitive mechanisms.

The comparison of samples produced from powder S with the addition of CaC_2 and of Y_2O_3 evidenced a slight decrease in the thermal conductivity of samples doped with CaC_2. On the contrary, previous studies [7] indicated that the more uniform the grain-size distribution and the lower amounts of secondary phases obtained by the addition of CaC_2, resulted in high thermal conductivity AlN ceramics. Moreover, results have also been reported [22] indicating that Ca segregated to the grain boundaries disrupted the connections among AlN grains. As the values of thermal conductivity depend on the effect of many parameters, it has to be considered that in this case powder S was rich in oxygen which could enhance the formation of CaO-based compounds. Thus, the second phases became more "wetting" and concentrated along the grain boundaries [22]. These factors are thought to be the main contributors to the observed decrease in thermal conductivity in CaC_2-doped samples, but the influence of the low amounts of porosity cannot be excluded. In most cases porosity is slightly higher in samples containing CaC_2 than in samples containing Y_2O_3.

5. Conclusions

The microstructure and thermal conductivity of AlN ceramics are strongly dependent on the purity level of the initial powders, the type and amount of additives and sintering conditions (temperature and time).

Values of thermal conductivity in the range of 50–200 $W m^{-1}K^{-1}$ were found to be dependent on microstructure and phase compositions.

Sintering in a nitrogen atmosphere with a very small oxygen partial pressure (graphite heaters and moulds) resulted in carbothermal nitridation which continuously decreased the overall oxide content. Consequently, the purity of AlN and thermal conductivity increased owing to the use of very pure powders, sintering atmosphere and high temperature/long soaking times. Only slight effects were measured that could be associated with the forming technique.

Acknowledgement

This research was carried out in the frame of the targeted project "Special Materials for Advanced

Technology" of the National Research Council of Italy.

References

1. K. SHINOZAKI, N. IWASE and A. TSUGE, FC Annual Report (1986) p. 16.
2. T. J. MORZ, *Ceram. Bull.* **70** (1991) 848.
3. P. BOCH, J. C. GLANDUS, J. JARRIGE, J. P. LECOMPTE and J. MEXAIN, *Ceram. Int.* **8** (1992) 34.
4. L. M. SHEPPARD, *Amer. Ceram. Soc. Bull.* **69** (1990) 1801.
5. G. A. S. LACK, *J. Phys. Chem. Solids* **34** (1973) 321.
6. R. R. LEE, *J. Amer Ceram. Soc.* **74** (1991) 2242.
7. Y. KUROKAWA, K. UTSUMI and H. TAKAMIZAWA, *J. Amer. Ceram. Soc.* **71** (1988) 588.
8. E. STREICHER, T. CHARTIER, P. BOCH, M. F. DENANOT and J. RABIER, *J. Europ. Ceram. Soc.* **6** (1990) 23.
9. S. RUCKMICH, A. KRANZMANN, E. BISCHOFF and R. J. BROOK, *J. Europ. Ceram. Soc.* **7** (1991) 335.
10. T. CHARTIER, E. STREICHER and P. BOCH, *J. Europ. Ceram. Soc.* **9** (1992) 231.
11. H. BUHR, G. MULLER, H. WIGGERS, F. ALDINGER, P. FOLEY and A. ROOSEN, *J. Amer. Ceram. Soc.* **74** (1991) 718.
12. J. P. LECOMPTE, J. JARRIGE and J. MEXMAIN, in "Progress in nitrogen ceramics", edited by F. C. Riley (Mortimus Nijholf, Boston, MA, 1973) p. 293.
13. A. BELLOSI and G. N. BABINI, in "Euro-Ceramics II, Vol. 3", edited by G. Ziegler and H. Hausner (Deutsche Keramische Ges., Köln, 1993) p. 1819.
14. K. KOMEYA, *Amer. Ceram. Soc. Bull.* **63** (1984) 1158.
15. A. KRANZMANN, P. GREIL and G. PETZOW, in "High tech ceramics", edited by P. Vincenzini (Elsevier, New York, 1987) p. 975.
16. K. WATARI, M. KAWAMOTO and K. ISHIZAKI, *J. Mater. Sci.* **26** (1991) 4727.
17. T. B. JACKSON, K. Y. DONALDSON and D-P. H. HASSELMAN, *J Amer. Ceram. Soc.* **73** (1990) 2511.
18. J. H. ENLOE, R. W. RICE, J. W. LAU, R. KUMAR and S. Y. LEE, *J. Amer. Ceram. Soc.* **74** (1991) 2214.
19. A. HAFIDI, M. BILLY and J. P. LECOMPTE, *J. Mater. Sci.* **27** (1992) 3405.
20. H. BUHR, A. THOMAS, G. MULLER, M. GUTHER, C. KOSTLER, A. ROOSEN and W. BOCKER, in "Euro-Ceramics II, Vol. 3", edited by G. Ziegler and H. Hausner (Deutsche Keramische Ges., Köln, 1993) p. 1843.
21. A. V. VIRKAR, T. B. JACKSON and R. A. CUTLER, *J. Amer. Ceram. Soc.* **72** (1989) 2031.
22. P. S. DE BARANDA, A. K. KNUDSEM and E. RUTH, *J. Amer. Ceram. Soc.* **76** (1993) 1751.
23. P. S. DE BARANDA, A. K. KNUDSEM and E. RUTH *J. Amer. Ceram. Soc* **76** (1993) 1761.
24. D. P. H. HASSELMAN and K. Y. DONALDSON, *Int J. Thermophys.* **11** (1990) 90.
25. L. FABBRI and E. SCAFE', *Rev. Sci. Instrum.* **63** (1992) 2008.

Received 16 November 1993
and accepted 25 February 1994